NASA TECHNICAL NOTE

NASA TN D-4384

NASA TN D-4384

ANALYTICAL DETERMINATION OF RADIAL INFLOW TURBINE DESIGN GEOMETRY FOR MAXIMUM EFFICIENCY

by Harold E. Rohlik

Lewis Research Center
Cleveland, Ohio

NATIONAL AERONAUTICS AND SPACE ADMINISTRATION • WASHINGTON, D. C. • FEBRUARY 1968

NASA TN D-4384

ANALYTICAL DETERMINATION OF RADIAL INFLOW TURBINE DESIGN GEOMETRY FOR MAXIMUM EFFICIENCY

By Harold E. Rohlik

Lewis Research Center
Cleveland, Ohio

NATIONAL AERONAUTICS AND SPACE ADMINISTRATION

For sale by the Clearinghouse for Federal Scientific and Technical Information
Springfield, Virginia 22151 – CFSTI price $3.00

ANALYTICAL DETERMINATION OF RADIAL INFLOW TURBINE DESIGN GEOMETRY FOR MAXIMUM EFFICIENCY

by Harold E. Rohlik

Lewis Research Center

SUMMARY

Radial turbine performance was examined analytically in order to determine optimum design geometry for various applications as characterized by specific speed. Five specific losses were calculated for various combinations of stator-exit flow angle, outlet- to inlet-diameter ratio, and the ratio of stator blade height to rotor-exit diameter. The losses considered were stator loss, rotor loss, tip-clearance loss, windage, and exit kinetic energy. Resulting static efficiencies ranged from 0.23 to 0.87 for a specific-speed range of 15 to 173 (0.12 to 1.34).

Turbine pressure ratio had no appreciable effect on optimum geometry except in the case of stator blade height. This variation occurred because of the changing ratio of rotor-exit area to stator-exit area which resulted from compressibility effects.

Curves of blade-jet speed ratio, stator-exit flow angle, tip-diameter ratio, and the ratio of stator blade height to rotor-inlet diameter are presented for maximum static efficiency over a wide range of specific speed. These curves permit the systematic selection of optimum turbine size and shape for a variety of turbine applications.

An exit diffuser of 0.6 effectiveness was examined for its effect on overall performance. The gain in static efficiency was appreciable except at very high specific speeds where a lower diffuser effectiveness or a different type of turbine would be required.

INTRODUCTION

Small radial inflow turbines are suitable for a variety of applications in aircraft, space vehicles, and other systems where compact power sources are required. Turbines of this type have a number of desirable characteristics, such as high efficiency, ease of manufacture, and sturdy construction. Since a radial turbine varies greatly in

form for the various applications, a correlation between the various design features and turbine losses is required in order to select optimum design features for a given design problem.

One parameter, used extensively in studies of this type, is specific speed, which includes the operating variables of turbine rotative speed, exit volume flow, and ideal specific work. These quantities, in most applications, are specified by the system conditions and by the pump, the compressor, the generator, or other equipment to be driven by the turbine. The value of specific speed provides a general index of flow capacity relative to work, with low values associated with relatively small flow passages and high values associated with relatively large flow passages. Specific speed has also been widely used as a general indication of achievable efficiency. The usual form of the specific-speed equation may be expanded to include a number of specific velocity-diagram and geometry parameters. Examination of these parameters shows that any number of combinations occur at any value of specific speed. These combinations encompass a considerable variation in turbine shape, speed, and pressure ratio. The significance of specific speed is discussed to some extent in references 1 and 2. Reference 3 describes a rather extensive experimental investigation of many radial turbine configurations and the effect of configuration change on performance. These discussions supply some of the desired information but do not provide a systematic examination of all the selections to be made in each turbine design.

The subject study considered the following losses: stator and rotor blading, rotor blade clearance, windage on the back face of the rotor, and exit velocity. These losses were examined in a mean-flow-path analysis for a wide range of turbine geometry with fixed values of rotor-tip blade speed. Stator-exit whirl varied with blade speed, flow angle, and rotor blade number in order to provide minimum rotor-entrance loss. Rotor reaction was held constant, and turbine-exit whirl was zero for all calculations. Independent variables were the stator flow angle, the ratio of stator blade height to rotor-exit diameter, and the exit- to inlet-diameter ratio.

Results of the study show the combination of geometric and velocity-diagram characteristics that results in maximum efficiency at any specific speed in the range investigated. The variations in stator, rotor, clearance, windage, and exit losses are also shown for maximum efficiency points in order to describe changes in internal flow conditions with specific speed. In addition, an exit diffuser with a fixed effectiveness was examined, and its effect on overall efficiency is discussed.

METHOD OF ANALYSIS

Approach

Specific speed is an expression commonly used to describe turbomachinery operating requirements in terms of shaft speed, exit volume flow, and ideal work and is, in equation form,

$$N_s = \frac{N\sqrt{Q_2}}{H^{3/4}} \tag{1}$$

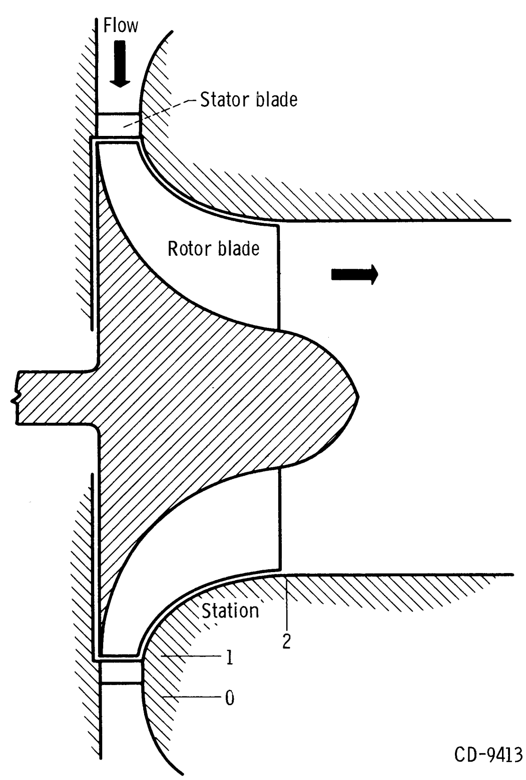

Figure 1. - Schematic cross section of radial inflow turbine.

Turbine station number designations are shown in figures 1 and 2, and all symbols are defined in appendix A. Substitution in this relation expands the expression to include several velocity-diagram and geometry ratios, as shown in equation (2):

$$N_s = \frac{60(2g)^{3/4}}{\sqrt{\pi}} \left(\frac{\Delta h}{\Delta h'}\right)_{id}^{3/4} \left(\frac{u_1}{V_j}\right)^{3/2} \left(\frac{V_2}{u_2}\right)^{1/2} \left(\frac{D_{2,m}}{D_1}\right)^{3/2} \left(\frac{h_2}{D_{2,m}}\right)^{1/2} \tag{2}$$

From this equation it is clear that any given specific speed can be achieved with a large number of combinations of these ratios. The problem, therefore, is to find the combination at each specific speed that will result in maximum efficiency.

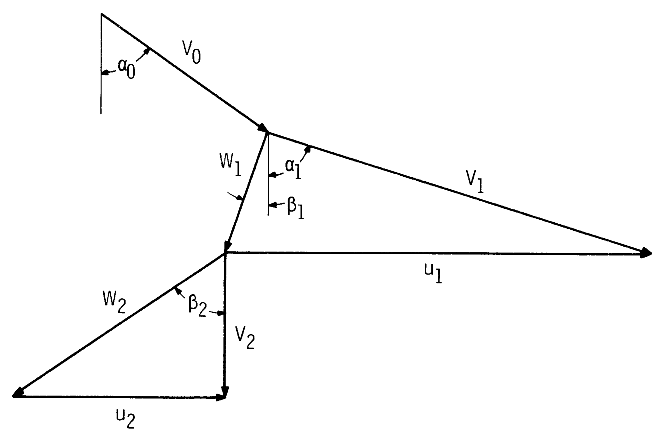

Figure 2. - Velocity diagram.

Five specific losses were calculated for each of many combinations of stator-blade-height to exit-diameter ratio $h_1/D_{2,m}$, stator-exit flow angle α_1, and exit- to inlet-diameter ratio $D_{2,m}/D_1$. These calculations result in a variety of combinations of the ratios shown in equation (2). The losses considered were those associated with stator-blade-row boundary layers, rotor-passage boundary layers, blade-shroud clearance, disk windage, and exit kinetic energy. Determination of relative velocities required certain assumptions relating these velocities to absolute gas and blade velocities. The first of these assumptions is at the inlet, where relative velocity was calculated with the "slip" factor determined in reference 4 for centrifugal compressors. The reference equation relates stator-exit whirl to blade speed and rotor blade number as follows

$$\left(\frac{V_u}{u}\right)_1 = 1 - \frac{2.0}{n} \tag{3}$$

where n is the number of rotor blades at the rotor inlet. The values for n were obtained from reference 5, wherein the blade number required to avoid zero blade surface

velocity is presented as a function of stator-exit flow angle. It was assumed herein that this rotor-inlet condition is optimum from the efficiency standpoint. All equations used in the analysis are shown in appendix B.

Rotor-exit relative velocity was then specified to be twice as large as the inlet relative velocity for consistent rotor reaction in all calculations and sufficiently high to assure low loss. Finally, the assumption of zero whirl leaving the turbine, along with the known exit blade velocity, results in a relative exit flow direction.

Initial calculations were made with a fixed rotor-inlet blade speed in terms of a critical velocity ratio $\left(u/V_{cr}\right)_1$ of 0.49, which corresponds to a blade speed of 500 feet per second (152.4 m/sec) with U.S. standard air at the turbine inlet. This assumption results in a limited range of turbine total pressure ratio and also of the ratio of stator throat area to rotor throat area. Additional calculations were therefore made to evaluate the effect of turbine pressure ratio on optimum geometry over the same range of specific speeds. This evaluation was done with calculations at rotor-inlet blade critical velocity ratios of 0.2 and 0.8.

Specific work for the main stream was calculated with whirl and blade speed at the rotor inlet. Net work was obtained by subtracting windage and clearance losses from the mainstream work. Ideal total specific work $\Delta h'_{id}$ based on total pressure ratio was taken as the sum of mainstream work, stator boundary-layer loss, and rotor boundary-layer loss. Ideal static specific work Δh_{id} based on inlet-total and exit-static pressures was then the sum of ideal total specific work and exit kinetic energy. Turbine efficiencies were determined with the net specific work and the ideal specific works.

Turbine-exit geometry was calculated as a function of the rotor-inlet flow conditions, the rotor loss, and the assumptions used in calculating relative velocities. Two limits were imposed on the exit diameters. The ratio of exit tip diameter to rotor-inlet diameter was limited to a maximum value of 0.7 to avoid excessive shroud curvature, and exit hub-tip diameter ratio was limited to a minimum of 0.4 to avoid excess hub blade blockage and loss.

Calculated Losses

Stator and rotor boundary layers. - Equations relating boundary-layer momentum thickness, blade geometry, energy level, and friction loss were presented in reference 6 for turbomachine blade rows. These equations were combined into a single equation for overall blade-row loss

$$e = E\left[\frac{\left(\frac{\theta_{tot}}{l}\right)\left(\frac{l}{c}\right)\sigma}{\cos \alpha_1 - \frac{t}{s} - \frac{\delta_{tot}}{s}}\right]\left(1 + \frac{\cos \alpha_{st}}{\sigma a}\right) \tag{4}$$

where e is the fraction of ideal kinetic energy that is lost.

Some of the terms in the equation were held constant in the solutions for stator and rotor losses. The following values were used as constants:

Term	Stator	Rotor
E	1.8	1.8
θ_{tot}/l	.003	.009
l/c	1.00	1.05
σ	1.4	(a)
t/s	.017	(a)
δ_{tot}/s	.008	(a)
α_{st}	(a)	18°
a	.5	(a)

[a]Calculated for each case.

The momentum thickness parameter θ_{tot}/l values are representative of subsonic axial turbines at high Reynolds numbers and were assumed to be valid for radial machines. The values selected establish the level of stator and rotor loss and, therefore, the level of efficiency obtainable. Variation in stator and rotor θ_{tot}/l values could result from changes in blade loading and Reynolds number and would change the overall level of turbine efficiency. Other quantities were calculated with approximate equations relating blade geometry to the independent variables α_1, $h_1/D_{2,m}$, and $D_{2,m}/D_1$.

Clearance. - Examination of the literature showed a variety of calculations for blade-shroud clearance loss. The ratio of loss to mainstream actual work varied from the ratio of clearance to passage height c/h to 1.3 c/h. Rotor blade clearance was assumed herein to reduce the mainstream work by the average ratio of clearance to passage height c/h. The ratios of clearance to clearance diameter were held constant as 0.0020 and 0.0025 at the rotor inlet and exit, respectively.

Windage. - Calculation of windage loss on the back face of the rotor was made with equation (5):

$$L_W = \frac{0.56\,\rho_1 u_1^3 D_1^2}{Re_w^{0.2}} \times 10^{-6} \tag{5}$$

This equation is a form of the power loss equation of reference 7 (p. 270).

Rotor exit. - The exit kinetic energy loss is simply the total of the energy associated with the leaving velocity:

$$L_E = \frac{V_2^2}{2gJ} \tag{6}$$

Procedure

The independent variables α_1, $h_1/D_{2,m}$, and $D_{2,m}/D_1$ were varied over the following ranges:

$$52^{\circ} < \alpha_1 < 83^{\circ}$$

$$0.04 < \frac{h_1}{D_{2,m}} < 0.68$$

$$0.2 < \frac{D_{2,m}}{D_1} < 0.6$$

Because efficiency and specific speed are of primary interest among the output variables, the preliminary calculations were evaluated in these terms. The wide range in input variables led to a large spread in efficiency at each value of specific speed. The upper envelope of the various curves of static efficiency against specific speed therefore represents the curve of optimum geometry for the range of specific speed covered. After determination of this curve, calculated points on and near the curve were examined for definition of optimum geometry.

RESULTS

Radial turbine performance was examined analytically to determine optimum design geometry for various applications. Initial calculations were made for constant rotor-inlet blade speed in terms of critical velocity ratio. Subsequent calculations were made at other blade speeds to determine the effect of internal Mach number level on optimum geometry.

Efficiency Characteristics

Blade critical velocity ratio at the rotor inlet was held constant at 0.49 for the first set of performance calculations with air entering the turbine at U.S. standard sea-level conditions. The combinations of input variables given in the section Procedure resulted in specific speeds from 15 to 173 (0.12 to 1.34) and static efficiencies ranging from 0.23 to 0.87. Figure 3 shows an example of the variation in static efficiency with specific-speed and diameter ratio for a constant stator-exit flow angle. The efficiency - specific-speed range is bounded by five curves. Two of these boundaries are the speci-

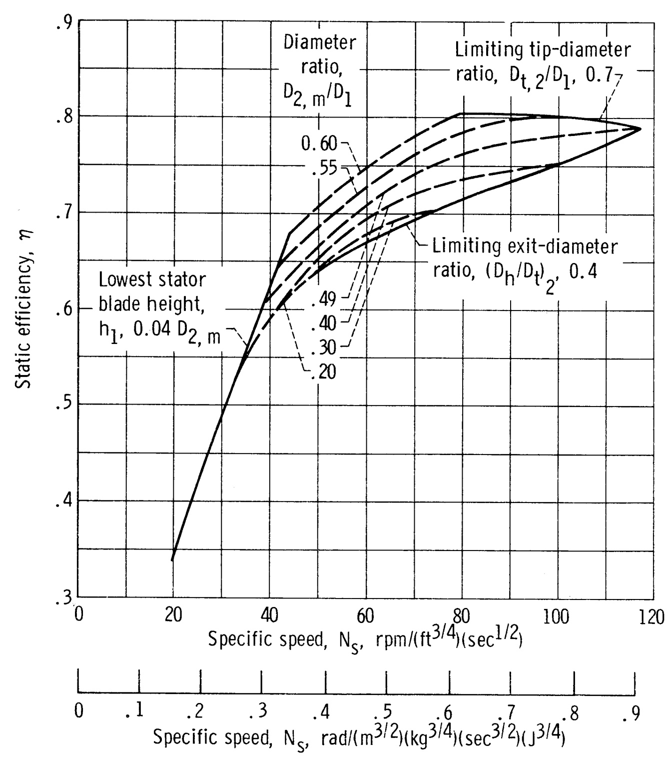

Figure 3. - Calculated performance with stator-exit flow angle α_1 of 68°.

fied diameter ratio limits as shown in figure 3. The intersection of these two curves sets the upper limit in specific speed for the given angle, 68°. The other boundaries were set by the input values of the independent variables.

Figure 4 shows similar areas for several other values of stator-exit flow angle. The envelope of the computed performance range peaks at a specific speed of 75 (0.58) with a static efficiency value of 0.87. This envelope may be referred to as the curve of maximum static efficiency or the optimum geometry curve. Examination of calculated points showed that exit hub-tip diameter ratio was 0.4 along the entire curve. The peak of the maximum static efficiency curve provides an interesting comparison with the experimental results obtained in the specific-speed investigation of reference 8. In that investigation, a single radial turbine rotor was operated with a number of stator blade rows of varying blade number and blade angle. This procedure provided a wide range of specific speeds through varying flow and specific work. The envelope of the static efficiency curves from reference 8 shows a peak of 0.87 at a specific speed of 82, although the design specific speed was 96. This peak is very close to the corresponding point on the maximum static efficiency curve of figure 4.

Total efficiency is also shown in figure 4 for combinations of variables corresponding to those of the maximum static efficiency curve. The maximum total efficiency was

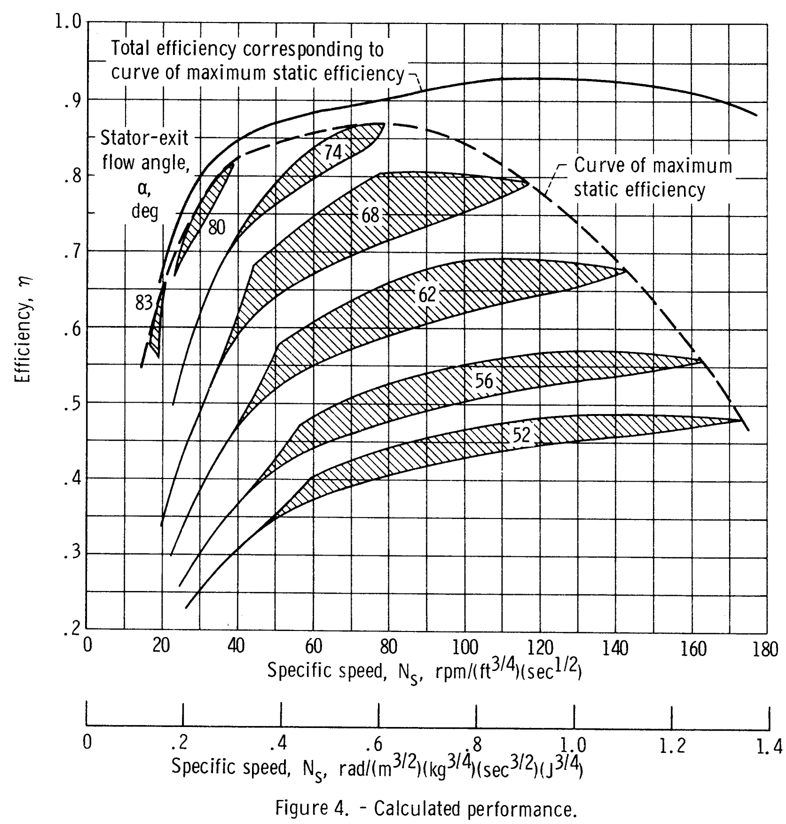

Figure 4. - Calculated performance.

0.93 at a specific speed of 120 (0.93) with values over 0.90 for a wide range of specific speed.

Examination of total efficiency for all calculated points showed that no values exceeded the total efficiency curve of figure 4 by more than 1 efficiency point. The geometry corresponding to the maximum static efficiency curve at all specific speeds can therefore be considered to be the geometry of maximum total efficiency as well.

Turbine Geometry

Turbine geometry was examined in detail for calculated points on and near the curve of maximum static efficiency. Several design parameters were then plotted as functions of specific speed to illustrate the changes in optimum turbine shape with application as represented by specific speed.

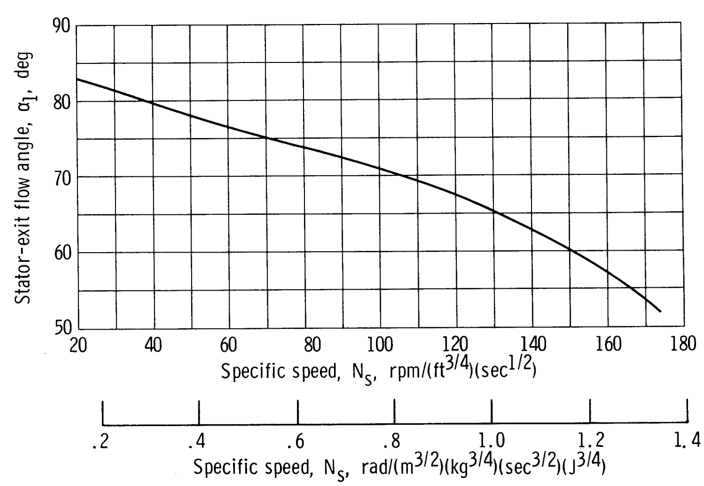

Figure 5. - Variation in stator-exit flow angle corresponding to maximum static efficiency with specific speed.

Figure 5 shows the variation in optimum stator-exit flow angle. A continuous decrease from 83° to 52° occurs as specific speed increases from 20 to 173 (0.16 to 1.34).

In figure 6, the ratio of stator blade height to rotor-inlet diameter increases from 0.012 to a peak of 0.159 as specific speed increases. This trend is in agreement with that of stator-exit flow angle and reflects the increase in stator flow area that accompanies the increase in volume flow and specific speed.

The ratio of exit tip diameter to rotor-inlet diameter is shown in figure 7. The low ratio at low specific speeds results from the high specific work relative to volume flow

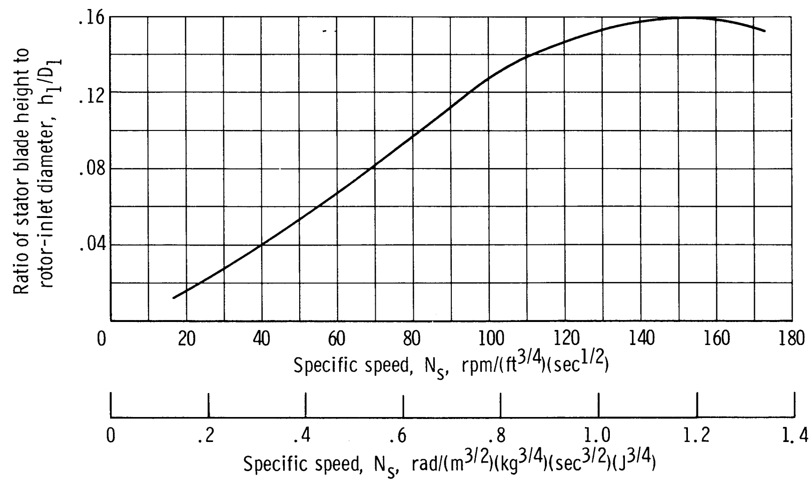

Figure 6. - Effect of specific speed on stator blade height for maximum static efficiency; rotor-inlet blade critical velocity ratio, $(u/V_{cr})_1$, 0.49.

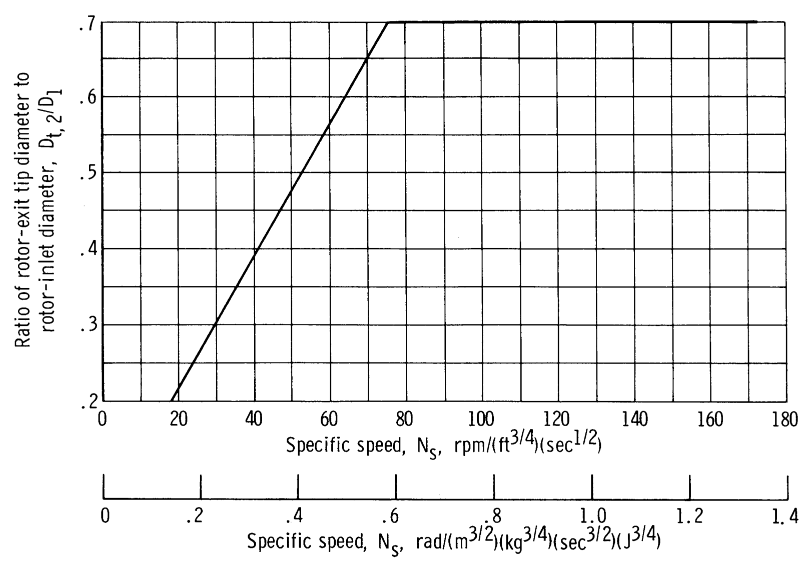

Figure 7. - Effect of specific speed on tip-diameter ratio corresponding to maximum static efficiency.

that produces the low specific speed values. This ratio increases rapidly to the specified limit at a specific speed of 75 (0.58).

The variation in blade-jet speed ratio with specific speed along the curve of maximum static efficiency is shown in figure 8. The nature of the calculations was such that the ratio of blade inlet tip speed to actual work was almost constant for all points calculated. Because blade-jet speed ratio includes ideal rather than actual work, the variation shown in figure 8 simply reflects the corresponding variation in static efficiency.

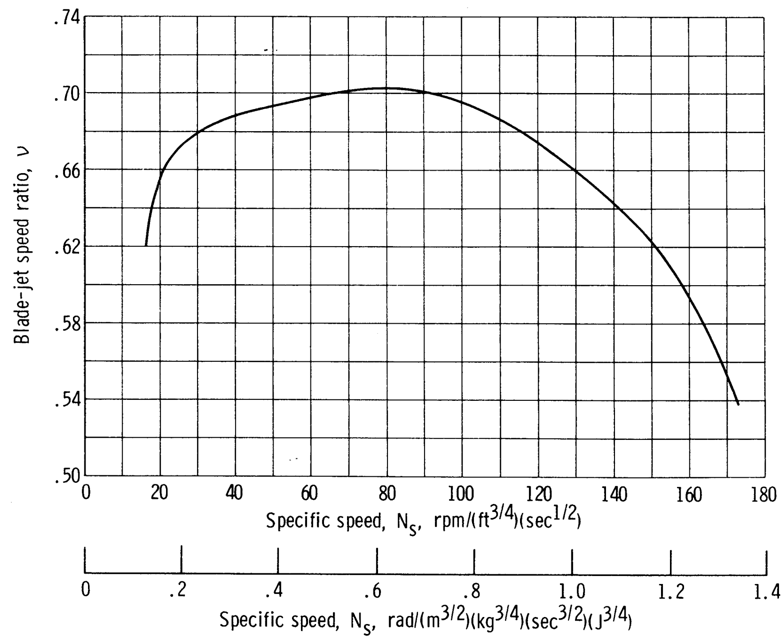

Figure 8. - Variation in blade-jet speed ratio corresponding to maximum static efficiency with specific speed.

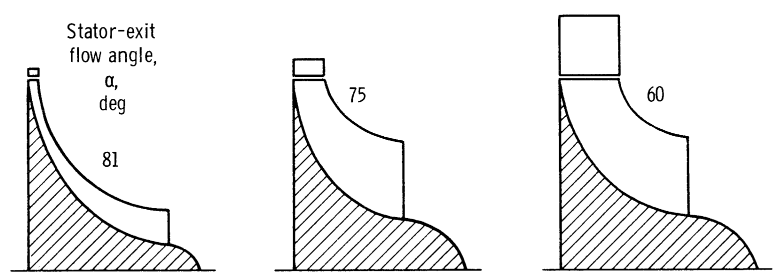

(a) Specific speed, 30 rpm per foot$^{3/4}$ per second$^{1/2}$ (0.23 rad/(m$^{3/2}$)(kg$^{3/4}$)(sec$^{3/2}$)(J$^{3/4}$)); blade-jet speed ratio, 0.68.

(b) Specific speed, 70 rpm per foot$^{3/4}$ per second$^{1/2}$ (0.54 rad/(m$^{3/2}$)(kg$^{3/4}$)(sec$^{3/2}$)(J$^{3/4}$)); blade-jet speed ratio, 0.70.

(c) Specific speed, 150 rpm per foot$^{3/4}$ per second$^{1/2}$ (1.16 rad/(m$^{3/2}$)(kg$^{3/4}$)(sec$^{3/2}$)(J$^{3/4}$)); blade-jet speed ratio, 0.62.

Figure 9. - Sections of radial turbines of maximum static efficiency.

Optimum geometric ratios obtained from the information presented to this point were used to prepare the turbine sections shown in figure 9. These sections correspond to the curve of maximum static efficiency at three values of specific speed. The axial lengths shown in figure 9 were selected as being reasonable for the diameter ratios shown. Determination of axial length as well as blade number and splitter blade length in a specific turbine design problem could best be made with a calculation of blade and end-wall gas velocities by a method such as that described in reference 8.

Internal Loss Variation

The distribution of loss among the five types calculated is shown in figure 10 for optimum geometry over the specific-speed range. The pattern of loss distribution results from the changing ratio of flow to specific work. At low values of specific speed, all friction losses are relatively large because of the high ratios of loss-generating areas to flow areas. At high specific speeds, the high velocities at the turbine exit made the leaving loss predominant.

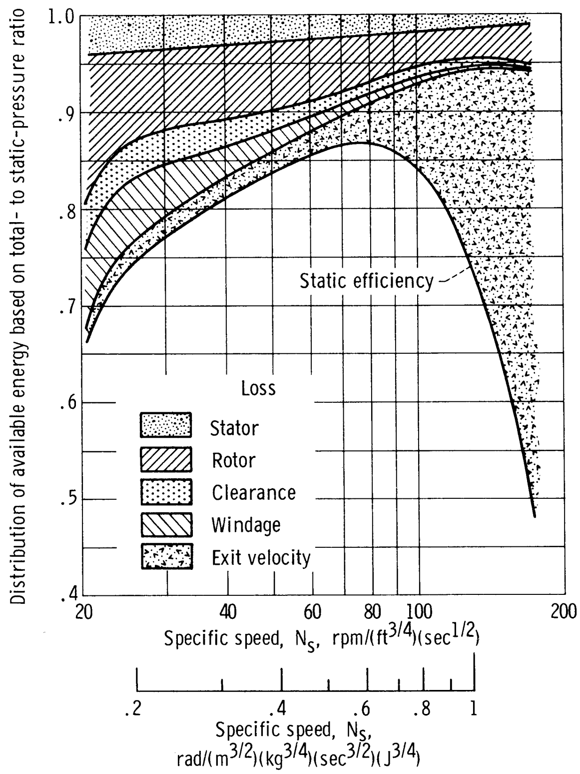

Figure 10. - Loss distribution along curve of maximum static efficiency.

Effect of Compressibility

The results of the initial calculations included a small variation in turbine pressure ratio and, therefore, a limitation on the usefulness of the results. The range of pressure ratio was extended by changing the level of all internal velocities. Rotor-inlet blade critical velocity ratios of 0.2 and 0.8 were specified, and all calculations were repeated for the same value of the input variables. All internal velocities varied in a con-

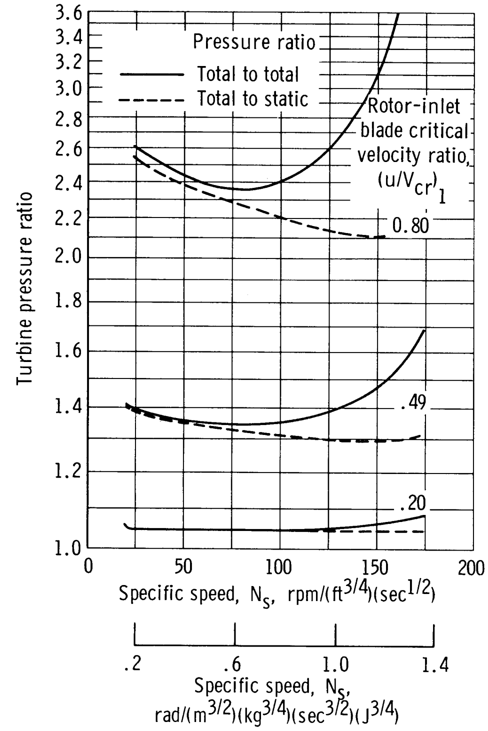

Figure 11. - Effect of specific speed on optimum turbine pressure ratios at three tip speeds.

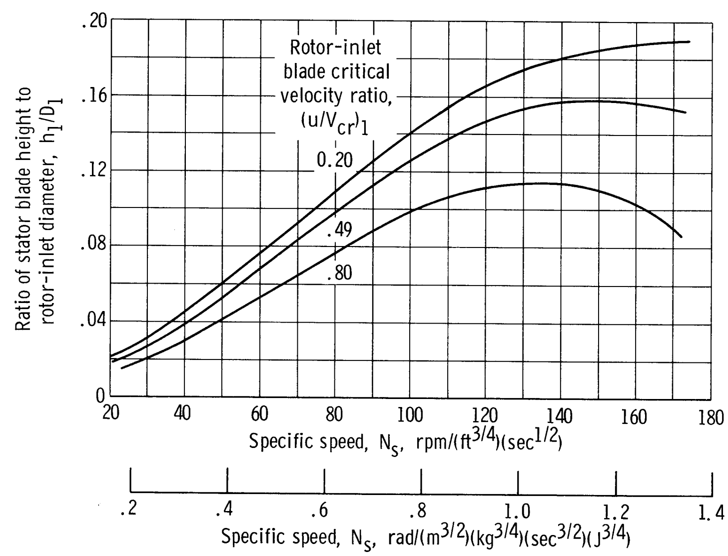

Figure 12. - Effect of specific speed on optimum stator blade height at three blade speeds.

sistent manner, and calculated efficiencies and optimum geometry parameters were almost identical for the three tip speeds with three notable exceptions. These exceptions were the turbine pressure ratios (total to total and total to static) and the stator blade height.

Figure 11 shows the variation of the turbine pressure ratios with specific speed and blade speed. The two kinds of pressure ratio for each blade speed diverge because exit velocity level increases with increasing specific speed. Relative velocities at the turbine exit become sonic at specific speeds above 160 in the highest wheel-speed case. This result indicates that total- to static-pressure ratios greater than 3.5 will result in exit losses greater than those calculated by the method of this analysis.

The effect of pressure ratio on stator blade height is shown in figure 12 for the three blade speeds calculated. The variation at all specific-speed levels results from a changing ratio of exit gas density to inlet gas density. Density decreases as the gas passes through the rotor because of the programmed reaction. Therefore, the ratio of exit area to inlet area increases with pressure ratio because of compressibility effects.

Effect of Exit Diffuser

The magnitude of turbine exit losses, particularly in the high specific-speed range, suggests the use of a diffuser to recover some of this energy and to increase overall static efficiency. Several points on the curve of maximum static efficiency were analyzed to determine the change in performance in the specific-speed range above 60 (0.46) that might be expected through use of a reasonable diffuser. Reference 9 includes performance measurements made with a radial turbine equipped with a diffuser over a range of operating conditions. This diffuser provided an average static pressure recovery or effectiveness of 60 percent of the diffuser-inlet velocity pressure and a total pressure loss of 25 percent of the inlet velocity pressure. These pressure-change fractions were held constant and were used to examine maximum static efficiency points at stator-exit flow angles of 52^{o}, 56^{o}, 62^{o}, 68^{o}, 71^{o}, 74^{o}, and 77^{o}. The results are shown in figure 13(a), where overall static and total efficiencies are shown as functions of specific speed. Portions of the optimum geometry curves of figure 4 (p. 9) are also shown for comparison. The specific-speed values are the same as those of figure 4, with H and Q referenced to rotor-exit conditions. The highest specific speed shows an overall total efficiency loss of 0.15 and an overall static efficiency increase of 0.19. The peak static efficiency and the peak total efficiency occur at specific speeds of 93 and 98 (0.72 and 0.76), respectively.

The values of H and Q in the specific-speed equation change appreciably when the turbine-diffuser combination is considered as a unit. The diffuser causes an increase in

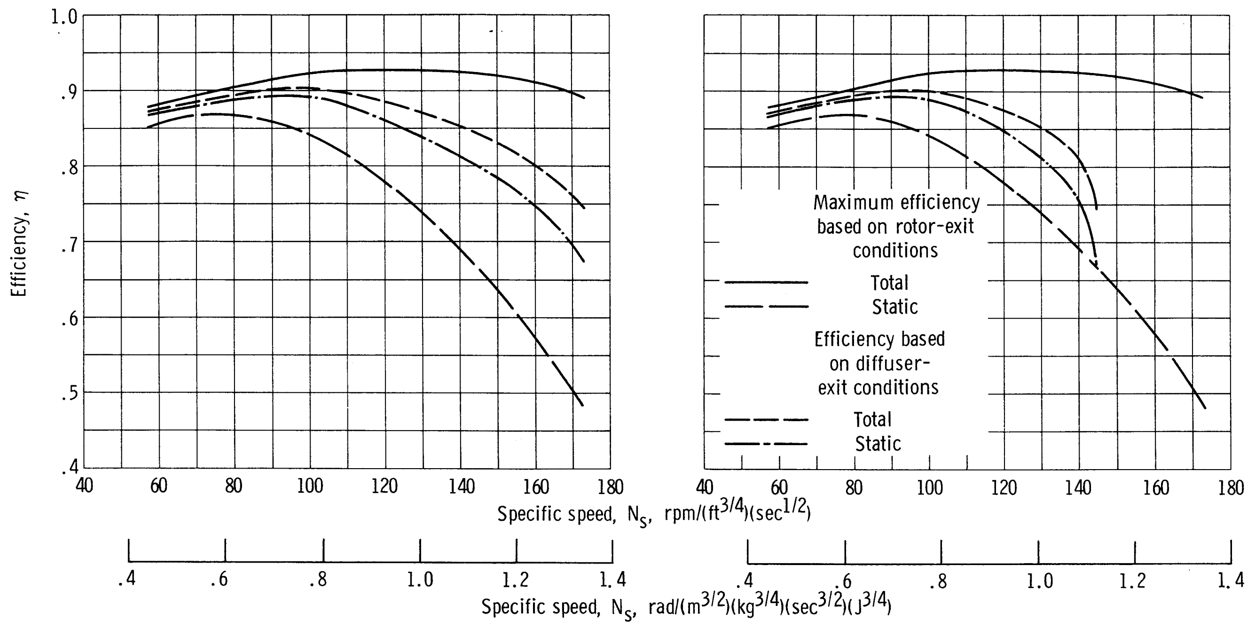

(a) All specific speeds referenced to turbine rotor exit, station 2.

(b) Specific speed for turbine-diffuser combination referenced to diffuser-exit conditions.

Figure 13. - Effect of diffuser on overall performance.

the overall work term H and a decrease in the flow term Q at the diffuser exit. Thus, the efficiency - specific-speed relation is changed to that shown in figure 13(b). Here again, the upper and lower curves are based on rotor-exit conditions and are portions of the maximum efficiency curves shown in figure 4 (p. 9). The two intermediate curves represent overall performance with diffuser-exit conditions used to calculate both efficiencies as well as new values for specific speed. The changes in volume flow rate Q and in ideal total work H combined to shift these curves from the pattern shown in figure 13(a) to lower values of specific speed. At high specific speeds, the diffuser-exit-based value actually decreases with increasing rotor-exit value. Thus, two pairs of turbine-diffuser efficiency values occur at specific speeds near 140 (1.08) for the diffuser effectiveness of 0.6. Operation with a diffuser at higher specific speeds would therefore require a lower effectiveness. In conclusion, this effect occurs only at high levels of specific speed, where efficiencies are considerably lower than the maximum achievable. A mixed-flow or axial turbine design would probably be selected for an application specifying such a high specific-speed level.

Application of Results

The results of the subject investigation provide a basis for the systematic selection of radial turbine size and shape for a wide variety of applications where maximum ef-

ficiency is an important consideration. The curves of blade-jet speed ratio, stator-exit flow angle, and tip-diameter ratio, used in that order, permit the rapid determination of turbine size and shape corresponding to zero exit whirl and good rotor reaction. Stator blade height is determined by a calculation that utilizes the appropriate working fluid properties, an appropriate slip factor, the rotor-inlet blade speed, and the weight flow dictated by the application. Blade number and inner-wall and outer-wall contours consistent with reasonable surface diffusion on all flow surfaces may then be established in an iterative manner with the quasi-orthogonal calculation of reference 10.

SUMMARY OF RESULTS

Radial turbine geometry was examined analytically to determine that geometry corresponding to maximum efficiency over a wide range of specific speeds. Pertinent geometry variables considered included stator-exit flow angle, rotor-exit- to inlet-tip-diameter ratio, ratio of stator blade height to rotor-tip diameter, and the rotor-exit hub-tip diameter ratio. The variation with specific speed in the optimum values of these geometric parameters as well as the corresponding blade-jet speed ratio, was determined. A basis was provided for the rapid selection of minimum-loss size and shape for any specific speed in the range used. In addition, pertinent analysis results can be summarized as follows:

1. The flow conditions and geometry parameters examined resulted in a range of specific speed from 15 to 173 (0.12 to 1.34). Maximum static and total efficiencies occurred at specific speed values of 75 and 120 (0.58 and 0.93), respectively.

2. Efficiency dropped rapidly with decreasing specific speed in the low specific-speed range. This drop resulted from the relatively high passage-boundary-layer, windage, and clearance losses associated with the high ratios of loss-generating areas to flow areas. At high specific speeds, the rotor exit loss was predominant because of the high volume flows.

3. The optimum geometry features described herein are essentially the same for both maximum static and maximum total efficiency. Also, optimum geometry at any specific speed was determined to be independent of pressure ratio except for one parameter, the ratio of stator blade height to rotor-inlet diameter. This ratio changes because of the density change across the rotor which is pressure-ratio dependent.

4. Exit-diffuser calculations with an effectiveness of 0.6 showed a shift in the peak static efficiency to a specific speed of 93 (0.72). The static efficiency with the diffuser was substantially higher than without the diffuser except at the higher levels of specific

speed based on the turbine-diffuser combination as a whole. In that area, a diffuser of lower effectiveness or a different type of turbine would be required for static efficiency higher than that of the radial turbine without a diffuser.

Lewis Research Center,
National Aeronautics and Space Administration,
Cleveland, Ohio, October 5, 1967,
120-27-03-13-22.

APPENDIX A

SYMBOLS

a	blade aspect ratio, h/C
C	blade chord, ft; m
C_p	specific heat, Btu/(lb)(^{o}R); J/(kg)(^{o}K)
c	blade-shroud clearance, ft; m
D	diameter, ft; m
E	energy factor
e	three-dimensional blade-row loss ratio
g	gravitational constant, 32.17 ft/sec
H	isentropic specific work based on total pressures, ft-lb/lb; J/kg
h	passage height, ft; m
Δh	turbine specific work, Btu/lb; J/kg
Δh_{id}	ideal turbine work based on inlet-total and exit-static pressures, Btu/lb; J/kg
Δh_y	turbine specific work (not corrected for windage and clearance losses), Btu/lb; J/kg
J	work-heat ratio, ft-lb/Btu
KE	kinetic energy, Btu/lb; J/kg
L	loss, Btu/lb; J/kg
l	blade mean camber length, ft; m
N	rotative speed, rpm
N_s	specific speed, $N\sqrt{Q_2}/H^{3/4}$, rpm/(ft$^{3/4}$)(sec$^{1/2}$); $\omega\sqrt{Q_2}/H^{3/4}$, (rad)(m$^{3/2}$)(kg$^{3/4}$)/(sec$^{3/2}$)(J$^{3/4}$)
n	number of rotor blades
p	pressure, lb/ft^2 abs; N/cm^2 abs
Q	volume flow rate, ft^3/sec; m^3/sec
R	gas constant, ft-lb/(lb)(^{o}R); J/(kg)(^{o}K)
Re	Reynolds number, $w/\mu r_t$
r	radius, ft; m
s	average rotor blade spacing, ft; m
T	temperature, ^{o}R; ^{o}K
t	blade thickness at trailing edge, ft; m
u	blade speed, ft/sec; m/sec
V	absolute gas velocity, ft/sec; m/sec
V_{cr}	local critical velocity, ft/sec; m/sec
V_j	ideal jet speed corresponding to total- to static-pressure ratio, ft/sec; m/sec
W	relative gas velocity, ft/sec; m/sec

w	mass flow, lb/sec; kg/sec
α	absolute gas flow angle (positive when whirl component of velocity is in direction of blade velocity), deg from meridional plane
β	relative gas flow angle (positive when whirl component of velocity is in direction of blade velocity), deg from meridional plane
γ	ratio of specific heats, 1.4
δ_{tot}	total displacement thickness, ft; m
η	efficiency
θ_{tot}	total momentum thickness, ft; m
μ	dynamic viscosity, lb/(ft)(sec); N/(sec)(m^2)
ν	blade-jet speed ratio
ρ	gas density, lb/ft^3; kg/m^3
σ	blade-row solidity, C/s
ω	angular velocity, rad/sec

Subscripts:

C	clearance
cr	critical
E	exit
h	hub
id	ideal, isentropic
m	mean or average
R	rotor
S	stator
st	stagger
T	turbine
t	tip
u	circumferential
W	windage
0	turbine stator inlet
1	stator exit and rotor inlet
2	turbine exit

Superscript:

'	total stagnation

APPENDIX B

EQUATIONS

The equations used in the calculation of turbine performance are listed herein in general order of solution. Certain quantities were held constant for each set of calculations. These quantities were inlet conditions p'_0 and T'_0; gas properties, γ, R, and C_p; blade speed u; and exit average diameter $D_{2,m}$. Specific results were calculated, as well as the dimensionless results presented in this report.

Independent variables α_1, $h_1/D_{2,m}$, and $D_{2,m}/D_1$ were used to arrive at a wide range of specific speeds. Some of the combinations of variables provided no realistic solutions because they exceeded the geometric limits of 0.7 on maximum tip-diameter ratio or 0.4 on minimum exit-hub- to tip-diameter ratio. Also, some of the extreme geometry combinations, particularly at low specific speeds, resulted in negative values of rotor loss when e_R values exceeded 1.0, because the boundary-layer thickness exceeded the flow-passage width and the loss equation was no longer valid. The equations are written for conventional units, and all solutions were obtained with U.S. standard air at the turbine inlet.

Stator-Exit Velocity Diagram

The stator-exit angle and rotor-inlet blade speed were specified as input. The exit velocity was computed by the equation

$$V_1 = \frac{u_1\left(1 - \frac{2}{n}\right)}{\sin \alpha_1} \tag{B1}$$

which relates the ratio of stator-exit tangential velocity to blade speed through the slip factor associated with the number of blades (ref. 4). The number of blades was computed by the equation

$$n = 0.3\left(\alpha_1 - 57\right)^2 + 12 \tag{B2}$$

which describes the curve of reference 5 that relates the stator-exit flow angle to the blade number required to avoid zero blade surface velocity. The rotor-inlet relative velocity was then computed by

$$W_1 = \sqrt{\left(\frac{2u_1}{n}\right)^2 + \left(V_1 \cos \alpha_1\right)^2} \tag{B3}$$

Stator Kinetic Energy Loss

This loss was obtained by the equation

$$L_S = e_S (KE)_{id, 1} \tag{B4}$$

where e_S is the stator loss coefficient. The ideal kinetic energy was computed by

$$(KE)_{id, 1} = \frac{(KE)_S}{1 - e_S} \tag{B5}$$

where

$$(KE)_S = \frac{V_1^2}{2gJ} \tag{B6}$$

The stator loss coefficient is related to the blade geometry and boundary-layer momentum thickness by equation (4) which was obtained from reference 6. With the constants assumed as reasonable values for this application, as noted in the section METHOD OF ANALYSIS, this equation becomes

$$e_S = \frac{0.0076}{\cos \alpha_1 - 0.025}\left(1 + \frac{\cos \alpha_{st}}{0.7}\right) \tag{B7}$$

The stator stagger angle was assumed to be the average of the inlet and exit flow angles

$$\alpha_{st} = \frac{\alpha_0 + \alpha_1}{2} \tag{B8}$$

where

$$\alpha_0 = \tan^{-1}\left[\frac{\sin \alpha_1}{4\left(\frac{h_1}{D_1}\right) + \cos \alpha_1}\right] \tag{B9}$$

which is the equation for an uncambered blade with an aspect ratio of 0.5.

Weight Flow

The turbine weight flow was calculated from the following continuity equation with previously calculated or input variables

$$w = \rho_0\left(\frac{p_1'}{p_0'}\right)\left(\frac{p}{p'}\right)_1^{1/\gamma} V_1 \cos \alpha_1(\pi D_1 h_1) \tag{B10}$$

where

$$\left(\frac{p}{p'}\right)_1 = \left[1 - \frac{(KE)_S}{C_p T_0'}\right]^{\gamma/\gamma-1} \tag{B11}$$

$$\frac{p_1}{p_0'} = \left[1 - \frac{(KE)_{id,1}}{C_p T_0'}\right]^{\gamma/\gamma-1} \tag{B12}$$

and

$$\frac{p_1'}{p_0'} = \frac{\frac{p_1}{p_0'}}{\left(\frac{p}{p'}\right)_1} \tag{B13}$$

Rotor-Exit Velocity Diagram

In the calculation of this diagram, it was assumed that

$$W_2 = 2W_1 \tag{B14}$$

This assumption was made to ensure reaction across the rotor sufficient to be consistent with low loss. Other diagram qualities were obtained by the equations

$$u_2 = u_1\left(\frac{D_{2,m}}{D_1}\right) \tag{B15}$$

$$V_2 = \sqrt{W_2^2 - u_2^2} \tag{B16}$$

$$\beta_2 = \sin^{-1}\left(\frac{u}{W}\right)_2 \tag{B17}$$

with the assumption of zero exit whirl.

Rotor Kinetic Energy Loss

This loss was calculated in a manner similar to that for the stator as follows:

$$L_R = e_R(KE)_{id,2} \tag{B18}$$

$$(KE)_{id,2} = \frac{(KE)_R}{1 - e_R} \tag{B19}$$

where

$$(KE)_R = \frac{W_2^2}{2gJ} \tag{B20}$$

the rotor loss coefficient took the form

$$e_R = \left(\frac{0.017\ \sigma_R}{\cos \beta_2 - 0.003\ n - 0.017\ \sigma_R}\right)\left(1 + \frac{1.9\ s}{h_1 + h_2}\right) \tag{B21}$$

This equation is again a form of equation (4) and includes the constants tabulated for the rotor in the section METHOD OF ANALYSIS. The solution requires an assumed value of h_2, which is subsequently compared iteratively with the computed value of equation (B30). Other equations required for the calculation of e_R include

$$\sigma_R = \frac{0.8\ D_{2,m}\left[\left(\frac{D_{2,m}}{D_1}\right) - 1\right]}{s} \tag{B22}$$

The constant 0.8 is used to obtain the approximate rotor blade chord as a function of rotor diameters. It includes an allowance for partial or splitter blades between the full blades

$$s = \frac{\pi D_{2,m}}{n}\left(\frac{1}{2}\frac{D_1}{D_{2,m}} + 1\right) \tag{B23}$$

where s is the average of the rotor-inlet and rotor-exit blade spacing.

Exit-State Conditions and Geometry

The exit-total and static fluid state conditions required for the continuity check at this point are as follows:

$$p'_2 = p'_0\left(1 - \frac{\Delta h_y + L_S + L_R}{C_p T'_0}\right)^{\gamma/\gamma-1} \tag{B24}$$

where Δh_y is the gas specific work output

$$\Delta h_y = \frac{u_1 V_1 \sin \alpha_1}{gJ} \tag{B25}$$

and

$$T'_2 = T'_1 - \frac{\Delta h_y}{C_p} \tag{B26}$$

$$\rho'_2 = \frac{p'_2}{RT'_2} \tag{B27}$$

$$\left(\frac{V}{V_{cr}}\right)_2 = \frac{V_2}{\sqrt{\frac{2\gamma g R T'_2}{\gamma - 1}}} \tag{B28}$$

$$\rho_2 = \rho'_2 \left[1 - \frac{\gamma - 1}{\gamma + 1}\left(\frac{V}{V_{cr}}\right)_2^2\right]^{1/\gamma - 1} \tag{B29}$$

The exit blade height can then be computed from continuity by

$$h_2 = \frac{w}{\pi D_{2,m} V_2 \rho_2} \tag{B30}$$

When this quantity is known, the exit-diameter ratio can be computed and compared with the limit specified

$$D_{2,t} = D_{2,m} + h_2 \tag{B31}$$

$$\left(\frac{D_h}{D_t}\right)_2 = \frac{D_{2,m} - h_2}{D_{2,m} + h_2} \tag{B32}$$

Windage Loss

The windage loss was computed by the equation

$$L_W = \frac{0.56\, \rho_1 \mu_1 D_1^2}{Re^{0.2}\ w} \times 10^{-6} \tag{B33}$$

which was taken from reference 7. The associated relations required for this solution are as follows:

$$Re = \left(\frac{\rho u D}{\mu}\right)_1 \tag{B34}$$

The density for this calculation was assumed to be the static value at the stator exit by the equation

$$\rho_1 = \frac{p_1'}{RT_0'}\left[1 - \frac{\gamma - 1}{\gamma + 1}\left(\frac{V}{V_{cr}}\right)_1^2\right]^{1/\gamma-1} \tag{B35}$$

where

$$V_{cr,1} = \sqrt{\frac{2\gamma g R T_0'}{\gamma + 1}} \tag{B36}$$

Clearance Loss

The loss due to the rotor blade clearance was computed with the assumption that this loss varies directly with average-clearance to blade-height ratio as follows:

$$L_c = \Delta h_y\left(\frac{c}{h}\right) \tag{B37}$$

where

$$\frac{c}{h} = \frac{1}{2}\left[\left(\frac{c}{h}\right)_1 + \left(\frac{c}{h}\right)_2\right] \tag{B38}$$

Using the specified input constants results in

$$c_1 = 0.002\ D_1 \tag{B39}$$

$$c_2 = 0.0025\ D_{2,t} \tag{B40}$$

Exit Loss

Exit loss is the kinetic energy corresponding to the leaving velocity expressed as

$$L_E = \frac{V_2^2}{2gJ} \tag{B41}$$

Overall Efficiency

The total and static efficiencies were calculated as follows:

$$\eta' = \frac{\Delta h}{\Delta h'_{id}} \tag{B42}$$

$$\eta = \frac{\Delta h}{\Delta h_{id}} \tag{B43}$$

where the work terms were obtained from

$$\Delta h = \Delta h_y - L_W - L_C \tag{B44}$$

$$\Delta h'_{id} = \Delta h_y + L_S + L_R \tag{B45}$$

$$\Delta h_{id} = \Delta h'_{id} + L_E \tag{B46}$$

Specific Speed

This parameter is defined as

$$N_s = \frac{N\sqrt{Q_2}}{H^{3/4}} \tag{B47}$$

and is computed by using

$$N = \frac{60u_1}{\pi D_1} \tag{B48}$$

$$H = J\ \Delta h'_{id} \tag{B49}$$

$$Q_2 = \pi D_{2,m} h_2 V_2 \tag{B50}$$

Efficiency Loss Items

The breakdown in efficiency caused by the various loss contributions was obtained as follows:

$$\left.\begin{aligned} \Delta\eta_S &= \frac{L_S}{\Delta h_{id}} \\ \Delta\eta_R &= \frac{L_R}{\Delta h_{id}} \\ \Delta\eta_C &= \frac{L_C}{\Delta h_{id}} \\ \Delta\eta_W &= \frac{L_W}{\Delta h_{id}} \\ \Delta\eta_E &= \frac{L_E}{\Delta h_{id}} \end{aligned}\right\} \tag{B51}$$

REFERENCES

1. Baljé, O. E.: A Study on Design Criteria and Matching of Turbomachines: Part A - Similarity Relations and Design Criteria of Turbines. J. Eng. Power, vol. 84, no. 1, Jan. 1962, pp. 83-102.
2. Wood, Homer J.: Current Technology of Radial-Inflow Turbines for Compressible Fluids. J. Eng. Power, vol. 85, no. 1, Jan. 1963, pp. 72-83.
3. Hiett, G. F.; and Johnson, I. H.: Experiments Concerning the Aerodynamic Performance of Inward Flow Radial Turbines. Paper No. 13 presented at the Thermodynamics and Fluid Mechanics Convention, Inst. Mech. Eng., London, Apr. 1964.
4. Stanitz, J. D.: Some Theoretical Aerodynamic Investigations of Impellers in Radial- and Mixed-Flow Centrifugal Compressors. Trans. ASME, vol. 74, no. 4, May 1952, pp. 473-497.
5. Jamieson, A. W. H.: The Radial Turbine. Gas Turbine Principles and Practice. Sir Harold Roxbee Cox, ed., D. Van Nostrand Co., Inc., 1955, Ch. 9.
6. Stewart, Warner L.; Whitney, Warren J.; and Wong, Robert Y.: A Study of Boundary-Layer Characteristics of Turbomachine Blade Rows and their Relation to Over-All Blade Loss. J. Basic Eng., vol. 82, no. 3, Sept. 1960, pp. 588-592.
7. Shepherd, D. G.: Principles of Turbomachinery. MacMillan Co., 1956.
8. Kofskey, Milton G.; and Wasserbauer, Charles A.: Experimental Performance Evaluation of a Radial-Inflow Turbine over a Range of Specific Speeds. NASA TN D-3742, 1966.
9. Futral, Samuel M., Jr.; and Holeski, Donald E.: Experimental Performance Evaluation of a 6.02-Inch (15.29-cm) Radial-Inflow Turbine with an Exit Diffuser. NASA TM X-1480, 1967.
10. Katsanis, Theodore: Use of Arbitrary Quasi-Orthogonals for Calculating Flow Distribution on a Blade-to-Blade Surface in a Turbomachine. NASA TN D-2809, 1965.

NASA-Langley, 1968 —— 3 E-3996

National Aeronautics and Space Administration
WASHINGTON, D. C.

OFFICIAL BUSINESS

FIRST CLASS MAIL

POSTAGE AND FEES PAID
NATIONAL AERONAUTICS AND
SPACE ADMINISTRATION

POSTMASTER: If Undeliverable (Section 158 Postal Manual) Do Not Return

"The aeronautical and space activities of the United States shall be conducted so as to contribute . . . to the expansion of human knowledge of phenomena in the atmosphere and space. The Administration shall provide for the widest practicable and appropriate dissemination of information concerning its activities and the results thereof."

—National Aeronautics and Space Act of 1958

NASA SCIENTIFIC AND TECHNICAL PUBLICATIONS

TECHNICAL REPORTS: Scientific and technical information considered important, complete, and a lasting contribution to existing knowledge.

TECHNICAL NOTES: Information less broad in scope but nevertheless of importance as a contribution to existing knowledge.

TECHNICAL MEMORANDUMS: Information receiving limited distribution because of preliminary data, security classification, or other reasons.

CONTRACTOR REPORTS: Scientific and technical information generated under a NASA contract or grant and considered an important contribution to existing knowledge.

TECHNICAL TRANSLATIONS: Information published in a foreign language considered to merit NASA distribution in English.

SPECIAL PUBLICATIONS: Information derived from or of value to NASA activities. Publications include conference proceedings, monographs, data compilations, handbooks, sourcebooks, and special bibliographies.

TECHNOLOGY UTILIZATION PUBLICATIONS: Information on technology used by NASA that may be of particular interest in commercial and other non-aerospace applications. Publications include Tech Briefs, Technology Utilization Reports and Notes, and Technology Surveys.

Details on the availability of these publications may be obtained from:

SCIENTIFIC AND TECHNICAL INFORMATION DIVISION

NATIONAL AERONAUTICS AND SPACE ADMINISTRATION

Washington, D.C. 20546